



Superficies y vacío

ISSN: 1665-3521

alex@fis.cinvestav.mx

Sociedad Mexicana de Ciencia y Tecnología
de Superficies y Materiales A.C.
México

Wuu, D. S.; Chan, C. C.; Horng, H.

Characterization of sputtered Ta-Ru thin films for ink-jet heater applications

Superficies y vacío, núm. 9, diciembre, 1999, pp. 180-183

Sociedad Mexicana de Ciencia y Tecnología de Superficies y Materiales A.C.

Distrito Federal, México

Available in: <http://www.redalyc.org/articulo.oa?id=94200948>

- How to cite
- Complete issue
- More information about this article
- Journal's homepage in [redalyc.org](http://www.redalyc.org)

[redalyc.org](http://www.redalyc.org)

Scientific Information System

Network of Scientific Journals from Latin America, the Caribbean, Spain and Portugal

Non-profit academic project, developed under the open access initiative

Characterization of sputtered Ta-Ru thin films for ink-jet heater applications

D. S. Wu, C. C. Chan,

Institute of Electrical Engineering, Da-Yeh University, Changhwa, Taiwan 515, ROCR.

H. Horng

Institute of Precision Engineering, National Chung Hsing University, Taichung, Taiwan 402, ROC

This paper discusses structural, electrical and oxidation characteristics of co-sputtered Ta-Ru alloy films on oxidized Si substrates. From x-ray examination, a Ta_1Ru_1 phase is formed and dominates in the compositions exceeding 54 at. % Ru content. The resistivity of the Ta-Ru thin films can reach a maximum of $\sim 320 \mu\Omega\text{-cm}$ in the composition range between 35 and 54 at. % Ru. After thermal treatment in air (600°C , 1 h), Ru-rich samples show a smaller increase in resistivity than Ta-rich ones. The observed preferential oxidation of Ta in the Ta-Ru samples can be further interpreted by thermodynamic calculations. The Ta-rich surface oxide is believed to be responsible for the passivating ability of Ru for oxidation at high temperatures. This results in the formation of Ru in metallic state, though the oxidation of Ta occurs. Finally, the Ta-Ru thin films without any additional passivation were fabricated in heater arrays to perform the inkjet lifetime test. A lifetime over 1×10^7 driving pulses can be achieved, which indicates Ta-Ru has high potential in thermal ink-jet applications.

1. Introduction

Thin films of tantalum is used in microelectronics industry in passive components for over 30 years [1]. Ta films are very stable, with a melting point of 3000°C , a tetragonal phase structure up to 750°C , and elastic stress behavior up to 600°C [2]. R. Duckworth [3] was the first who tried to improve the properties of Ta films for thin-film resistors by alloying Ta with Al. An unique application of thin-film resistors can be considered to be the thermal ink jet printers [4,5]. The films must have sufficient resistivity ($>150 \mu\Omega\text{-cm}$) for making heaters of controllable thicknesses. The thermal ink-jet devices require resistive films having unusually high structural, electrical and chemical stabilities since they are employed in modest size arrays for ejecting ink droplets on demand: all the devices in an array must function properly for several hundred million cycles or more for useful head reliability. The most popular resistor materials that are currently in use for thin film heaters include sputtered Ta-Al alloys [4], heavily doped silicon [6] and sputtered HfB_2 [7]. All of the heater films, typically 60-100 nm thick, are expected to survive billions of thermal cycles to $\sim 400^\circ\text{C}$ at heating rates of $\sim 10^8^\circ\text{C/s}$. The resistor materials described above are not always satisfactory in duration or stability for an application to a permanently used printhead.

In this paper, the characterization of Ta-Ru sputtered alloys are studied. Tantalum and ruthenium are selected from a point of view of substances, which have high heat resisting, mechanical strength and chemically stable properties. Coexistence of the two elements at the specific composition rates is expected to make adjustable resistivity and increase the adhesion and toughness. The structural and electrical properties of the Ta-Ru thin films over a wide range of compositions are investigated. The oxidation behavior, which is important to manufacturing reliable ink-jet products, will also be described. The results show that Ta-Ru films possess a wide range of properties that are suitably stable for advanced ink-jet printheads.

2. Experimental

Thin films of Ta-Ru were deposited onto thermally oxidized Si(100) wafers by co-sputtering. Details of the deposition system employed in this work have been reported previously [8]. Both Ta and Ru targets with up to 99.95% purity were mounted on two 100-mm-diam sputtering cathodes. The substrate was preheated to 150°C for 1 h at the base pressure ($\sim 2 \times 10^{-5}$ Pa) and then kept at the temperature for deposition. In these experiments, the rf power applied to the Ta target was fixed at 300 W while the dc power to the Ru target was adjust to the desired alloy composition. The Ar sputtering gas used was 99.999% purity and the pressure was maintained at 2 Pa during the deposition.

Crystallinity of the Ta-Ru samples was investigated by x-ray diffraction (XRD) with $\text{Cu } K_\alpha$ radiation. The composition and chemical state of the films were determined by x-ray photoelectron spectroscopy (XPS) using a $\text{Mg } K_\alpha$ radiation source. The composition profile was determined by Auger electron spectroscopy (AES) in combination with Ar sputter etching. A four-point-probe mapping system was used in measuring the sheet resistance of the films. All the Ta-Ru samples used were about 150-200 nm thick with uniformity within 2%.

For the unpassivated thermal-bubble transducer, a p-type (100) Si wafer with 1.7- μm -thick thermal oxide was used as substrate. Over the thermal barrier, the Ta-Ru film (~ 100 nm thick) was deposited as a heater material, and then a layer of Al film was deposited as a conductor film. The unpassivated heater array (without any additional coatings) can be prepared via standard photolithography and dry etching processes for Al and Ta-Ru. The testing apparatus comprises a pair of probes, an x-y moving station, a microscope lens, an image camera including a monitor, and the most important, a dc pulse generator with the drop counter. During test, firing frequency and pulse width were set to 1 kHz and 3 μs , respectively. A droplet of de-ionized water was put on the heater surface as an indicator of bubble formation (namely, open-pool test) [9].

3. Results and Discussion

Table 1 illustrates the x-ray diffraction and resistivity data of the Ta-Ru samples with various alloy compositions. β -Ta phase was found to be dominant in the Ta-enriched films. With increasing the Ru content, the β -Ta (432) reflection was diminished and the β -Ta (212) peak was gradually broadened and mixed with the tetragonal Ta_1Ru_1 (101) peak. The Ta_1Ru_1 (101) phase exists dominating in the compositions over 54 at. % Ru. Further increasing the Ru content results in the formation of Ru (002) phase, which is dominant in the pure Ru sample. On the other hand, samples with small Ru additions show no evident effect on resistivity, as compared with the pure Ta film. With increasing the Ru contents over 13 at. %, the resistivity begin to rise and reach a maximum of $\sim 320 \mu\Omega\text{-cm}$ at a composition of ~ 46 at. % Ru. The trend is reasonable because the Ru atoms can be regarded as impurity and diminish the degree of crystalline perfection of the pure metal. The impurity atom will, in general, carry an effect of electric charge different from that of the parent metal; it will therefore hinder the movement of the electrons and increase the resistivity [10]. The observed composition effect on the Ta-Ru resistivity correlates well with the x-ray measurement results.

Table 1: X-ray diffraction and resistivity data of Ta-Ru films with various compositions. Resistivity data for samples after 700°C annealing (in air for 1 hr) are provided.

$\text{Ta}_{1-x}/\text{Ru}_x$	Phase Identified	Resistivity ($\mu\Omega\text{-cm}$)	
		as-deposited	after annealing
1/0	(212) βTa^{**} , (432) βTa^*	140	$>1 \times 10^6$
0.87/0.13	(212) βTa^{**} , (432) βTa^*	154	$>1 \times 10^6$
0.78/0.22	(212) βTa^{***}	261	2386
0.65/0.35	(212) βTa^{**} , (101) $\text{Ta}_1\text{Ru}_1^{+**}$	293	792
0.54/0.46	(101) $\text{Ta}_1\text{Ru}_1^{+**}$	320	641
0.46/0.54	(101) Ta_1Ru_1^*	265	320
0.39/0.61	(101) $\text{Ta}_1\text{Ru}_1^{**}$, (202) $\text{Ta}_1\text{Ru}_1^{+**}$	197	235
0.34/0.66	(101) $\text{Ta}_1\text{Ru}_1^{***}$, (202) Ta_1Ru_1^*	183	126
0.13/0.87	(002) Ru^*	78	120
0/1	(002) Ru^{***} , (004) Ru^*	47	3546

Intensity of x-ray peak $*** > ** > * > ^+ > ^*$

Also illustrated in Table 1 is the resistivity data of Ta-Ru alloys after 600°C thermal treatment in air for 1 h. It was found that the resistivity increased obviously for the Ta-enriched films or the pure Ru metal. Only a limited increase in resistivity was observed as the Ru composition varies from 0.54 to 0.85. As concerning the thermal ink-jet application, the oxidation behavior of the Ru-rich samples is of great interest. Fig. 1 shows the XRD pattern for the as-deposited $\text{Ta}_{0.46}\text{Ru}_{0.54}$ sample, as compared with that of the annealed sample. After oxidation, the Ta_1Ru_1 (101) peak disappeared and the Ru (002) and (004) peaks were observed. The emergence of Ta (101) and (202) peaks reveals that Ta has the tendency toward oxidation. The formation of Ta oxide could contribute to the measured variation in resistivity data for the Ta-enriched samples after oxidation.

The surface morphology is extremely important in consideration of the ink-jet heater material. The AFM topographies of the annealed $\text{Ta}_{0.46}\text{Ru}_{0.54}$ film compared with that of the as-deposited film are shown in Fig. 2. Although the surface rearrangement and oxidation occur, the surface still appears smooth. The average roughness increases from 4.01 nm to 9.35 nm over the relatively wide area of $10 \mu\text{m} \times 10 \mu\text{m}$. Moreover, the annealed $\text{Ta}_{0.46}\text{Ru}_{0.54}$ sample can be interpreted by the AES analyses as shown in Fig. 3. It can be found that the as-deposited Ta-Ru samples have 1 at. % oxygen uniformly distributed throughout the films. Due to its reactive nature, even Ta-Ru sputtered at a base pressure of $2\text{-}3 \times 10^{-5}$ Pa getters some oxygen. After thermal treatment, there is 14 at. % oxygen uniformly distributed throughout the film. This suggests that oxidation of the entire layer will occur during the heat treatment. Fig. 4 presents the cross-sectional view of the annealed $\text{Ta}_{0.46}\text{Ru}_{0.54}$ sample by transmission electron microscopy. It correlates well with the Auger result that the tantalum and

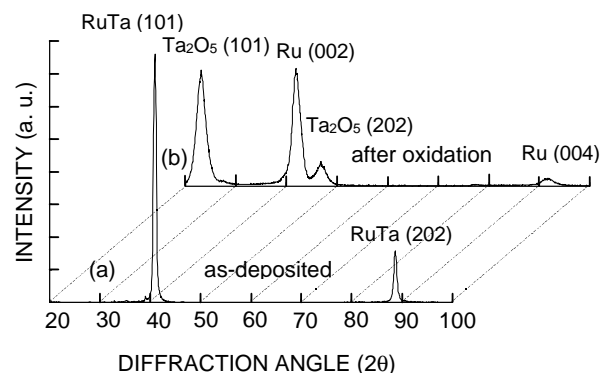


Fig. 1. X-ray diffraction patterns of (a) as-deposited and (b) annealed $\text{Ta}_{0.46}\text{Ru}_{0.54}$ samples. The annealing process used is 600°C in air for 1 h.

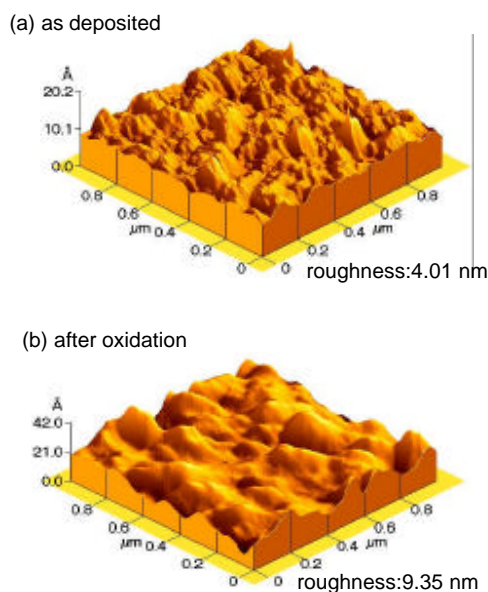


Fig. 2. AFM topographies of (a) as-deposited sample and (b) the $\text{Ta}_{0.46}\text{Ru}_{0.54}$ film annealed at 600°C in air for 1 h.

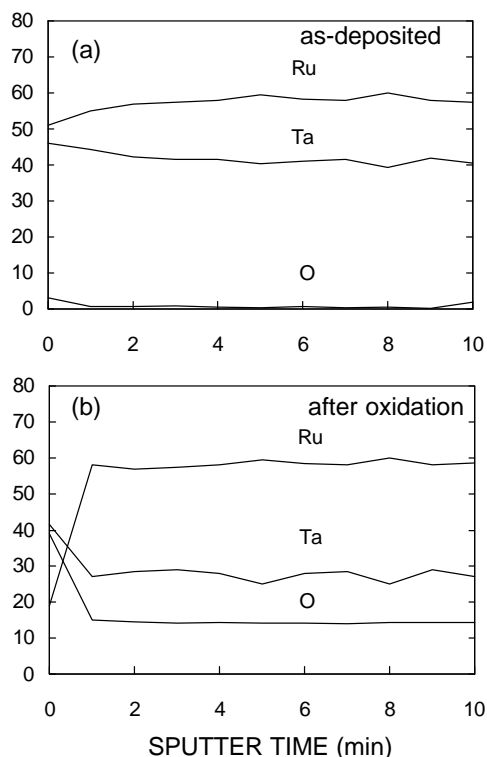


Fig. 3. In-depth Auger profiles of (a) as-deposited sample and (b) the $\text{Ta}_{0.46}\text{Ru}_{0.54}$ film annealed at 600°C in air for 1 h.

oxygen concentrations pile up slightly near the film surface as depicted in Fig. 3(b). As the oxidation proceeds through the Ta-Ru film, a large amount of metallic Ta may migrate to the subsurface region to form the Ta oxide. The Ta-rich surface oxide is believed to be responsible for the passivating ability of the Ru atoms with respect to oxidation at high temperatures.

To further study the oxidation behavior, the annealed $\text{Ta}_{0.46}\text{Ru}_{0.54}$ sample was examined by XPS to identify the binding energy configuration. Two peaks of Ta $4f_{7/2}$ transitions at 22.87 and 26.74 eV were observed in the sputtered clean surface. The peak position at 26.74 was in good agreement with those reported previously for the Ta $4f_{7/2}$ peak from Ta_2O_5 [11,12]. On the other hand, the Ru $3d_{5/2}$ core level of the sputtered clean surface was found to be 280.17 eV, which correspond to the metallic ruthenium [11,13]. The observed preferential oxidation of Ta in the Ta-Ru samples can be interpreted thermodynamically. The standard Gibbs energy of formation (DG°) for Ta_2O_5 and RuO_2 at 873K is calculated to be -677338 and -154143 J/mol, respectively [14]. Since Ta has a higher negative DG° of metal oxide in comparison with Ru, preferential oxidation of Ta in Ta-Ru film would be reasonable. As the oxidation proceeds to the $\text{Ta}_{0.46}\text{Ru}_{0.54}$ film, a large amount of metallic Ta migrates to the subsurface region to form the Ta oxide. It can be further supported by the Auger result that the tantalum and oxygen concentrations pile up near the film surface as depicted in Fig. 3(b). The Ta-rich surface oxide is believed to be responsible for the passivating ability of the Ru atom toward oxidation at high temperatures. This results in the Ru of the metallic state. For the ink-jet heater application, the Ta-Ru samples were fabricated in arrays ($\sim 60 \times 60 \mu\text{m}^2$) to perform the open pool test [9]. Testing began when the heater arrays were submerged in de-ionized water which forms the basis of a variety of commercial inks. Pulse currents were applied to the heater arrays and were adjusted so that heat conduction through the samples to the water was sufficient to produce vapor bubbles along the Ta-Ru heater surface. Samples were typically subjected to $3\mu\text{s}$ square pulses at 1 kHz. Fig.

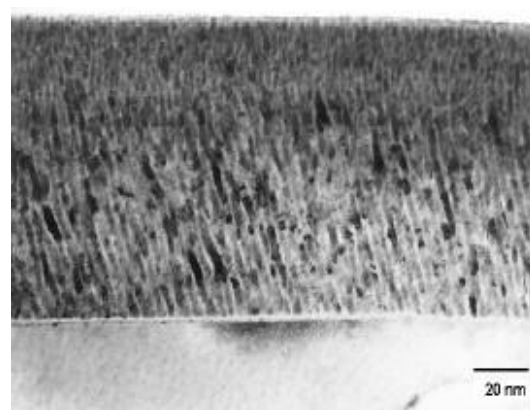


Fig. 4. Cross-sectional transmission electron micrograph of the $\text{Ta}_{0.46}\text{Ru}_{0.54}$ sample annealed at 600°C in air for 1 h.

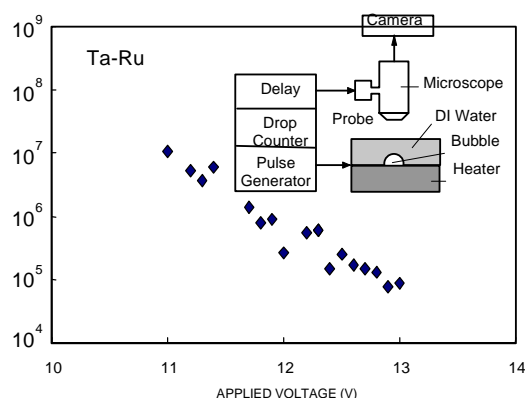


Fig. 5. Relationship between applied voltage and droplets to failure of Ta-Ru thin film heaters

5 depicts the test result (sample with 54 at. % Ru content) in semi-log scale where the number of droplets to failure is inversely exponential versus the applied voltage. The total resistance of the testing device is $30.5 \pm 0.2 \Omega$. The lowest voltage that can generate a thermal bubble is 9.1 ± 0.1 V.

Two typical failure modes of unpassivated heater (without any additional coatings) can be observed. One general failure mode is the heater element broken cross the pulse current direction due to the over-driven condition. However, under a long-term testing in a quite low voltage, the power applied to the device can generate enough energy to vaporize the water on the heater surface over 1×10^7 pulses. But the center of the heater element will be attacked due to the cavitation force. This failure mode will not appear in the completely processed device, since the dry film pattern, which acts as an ink barrier, will shift the bubble collapse point to the edges of heater due to the surface tension between the bubble and the barrier walls.

4. Conclusions

The characteristics of Ta-Ru alloy films were evaluated for thin-film heater materials. For Ru contents higher than 46 at. %, the Ta_1Ru_1 phase forms and presents the {101} orientation. After oxidation, the Ru-rich samples are more stable in resistivity than the Ta-rich samples. Since Ta has a higher negative DG° of metal oxide in comparison with Ru, preferential oxidation of Ta in Ta-Ru film is reasonable and results in the Ru being in the metallic state. The data presented suggests that Ta-Ru alloys at a composition near 54 at. % Ru is suitable as the heater material for future ink jet applications.

Acknowledgements

This research was supported by the National Science Council of ROC under Contract No. NSC 87-2215-212-001. The authors are grateful to Dr. Y. Y. Wu of OES/ITRI, Taiwan, for insightful discussions. Thanks are also expressed to S. Y. Lee of National Sun Yat-Sen University,

Kaohsiung, Taiwan, for her efforts in x-ray diffraction measurements.

References

- [1] W. D. Westwood, N. Waterhouse and P. S. Wilcox, *Tantalum Thin Films* (Academic, London, 1975), p. 406.
- [2] L. A. Clevenger, A. Mutscheller, J. M. E. Harper, C. Cabral, Jr. and K. Barmark, *J. Appl. Phys.* **72**, 4918 (1992).
- [3] R. Duckworth, *Trans. MRC-Sputtering Conf.*, Brighton, London, 1969, p. 60.
- [4] J. S. Aden, J. H. Bohorquez, D. M. Collins, M. D. Douglas, A. Garcia and U. E. Hess, *Hewlett-Packard J.* **45**, 41 (1994).
- [5] J. H. Jou, L. Hsu and L. S. Chang, *Thin Solid Films* **201**, 253 (1991).
- [6] W. G. Hawkins, US Patent No. 4,532,530 (1985).
- [7] J. M. Eldridge, A. R. Forouhi, G. L. Gorman and J. O. Moore, *J. Electrochem. Soc.* **137**, 3905 (1990).
- [8] D. S. Wu, C. C. Chan, R. H. Horng, W. C. Lin, S. L. Chiu and Y. Y. Wu, *Appl. Surf. Sci.* **144**, 315 (1999).
- [9] L. S. Chang, P. L. Gendler, and J. H. Jou, *J. Materials Sci.* **26**, 1882 (1991).
- [10] L. I. Maissel, in *Handbook of Thin Film Technology*, edited by L. I. Maissel and R. Glang (McGraw-Hill, New York, 1983), p. 13-3.
- [11] J. H. Moulder, W. F. Stickle, P. E. Sobol, and K. D. Bomben, in *Handbook of X-ray Photoelectron Spectroscopy*, edited by J. Chastain and Jr., R. C. King (Physical Electronics, Minnesota, 1984).
- [12] S. Badrinarayanan and S. Sinha, *J. Appl. Phys.* **69**, 1141 (1991).
- [13] J. Hrbek, D. G. V. Campen, and I. J. Malik, *J. Vac. Sci. Technol.* **A13**, 1409 (1995).
- [14] C. B. Alcock, in *CRC Handbook of Chemistry and Physics*, edited by D. R. Lide (CRC, Florida, 1995), p. 5-72.